

## Supplementary Material for

# **Moss-like CoB/CeO<sub>2</sub> heterojunction as an efficient electrocatalyst for oxygen evolution reaction under alkaline conditions**

Weijie Fang<sup>1,a</sup>, Chaofan Liu<sup>1,a</sup>, Jiang Wu<sup>1,\*</sup>, Weikai Fan<sup>1</sup>, Le Chen<sup>4</sup>, Zaiguo Fu<sup>1</sup>, Lin Peng<sup>2</sup>, Ping He<sup>1</sup>, Jia Lin<sup>2,\*</sup>,  
Zhongwei Chen<sup>3,\*</sup>

1. College of Energy and Mechanical Engineering, Shanghai University of Electric Power, Shanghai 200090, China
2. College of Mathematics and Physics, Shanghai University of Electric Power, Shanghai 200090, China
3. Dalian Institute of Chemical Physics, Chinese Academy of Sciences, Dalian 116023, China
4. Shanghai Institute of Special Equipment Inspection and Technical Research, Shanghai 200062, China

<sup>a</sup> These authors contributed to the work equally and should be regarded as co-first authors.

\*Corresponding authors

Jiang Wu (Ph.D., Professor)

Mobile: +86-13371896217

E-mail Address: wjcf2002@163.com

Postal Address: No. 2103 Ping liang Road, Shanghai 200090, People's Republic of China.

Jia Lin

E-mail Address: jlin@shiep.edu.cn

Postal Address: No. 2103 Pingliang Road, Shanghai 200090, China.

Zhongwei Chen

E-mail Address: zwchen@dicp.ac.cn

Postal Address: No. 457 Zhongshan Road, Dalian 116023, China.

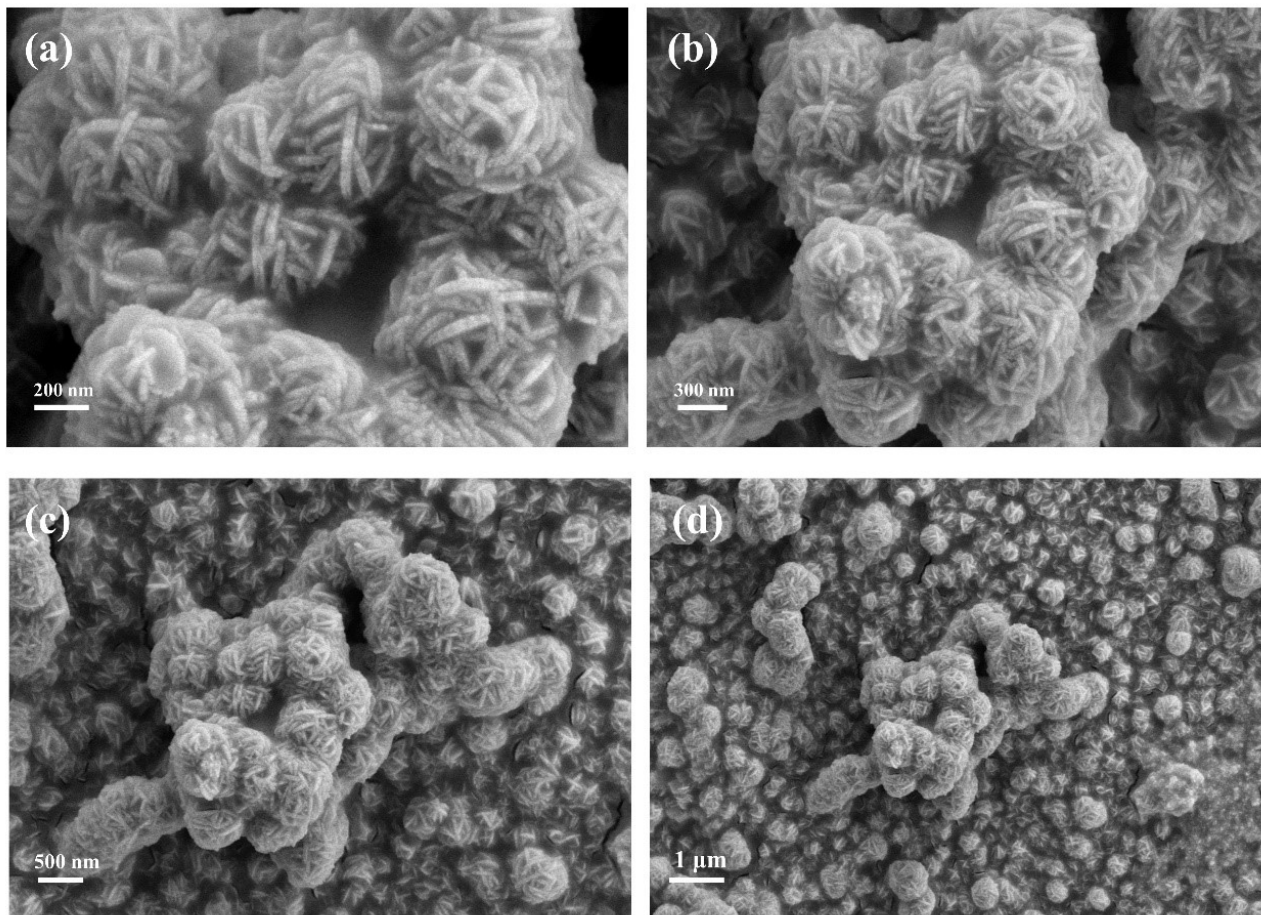


Figure S 1. SEM images of CoB at (a) 200 nm, (b) 300 nm, (c) 500 nm, and (d) 1  $\mu\text{m}$ .

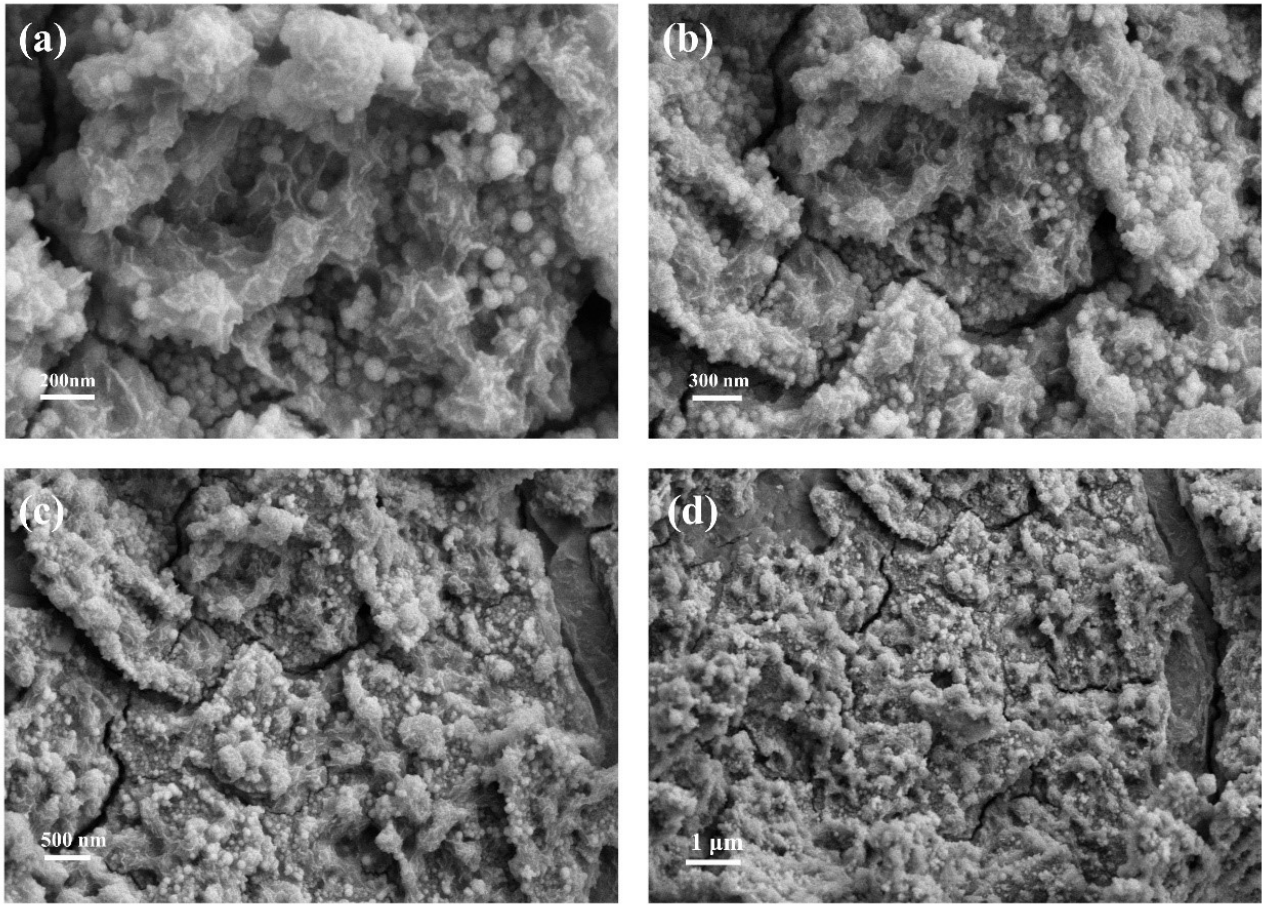


Figure S 2. SEM images of CeO<sub>2</sub> at (a) 200 nm, (b) 300 nm, (c) 500 nm, and (d) 1 μm.

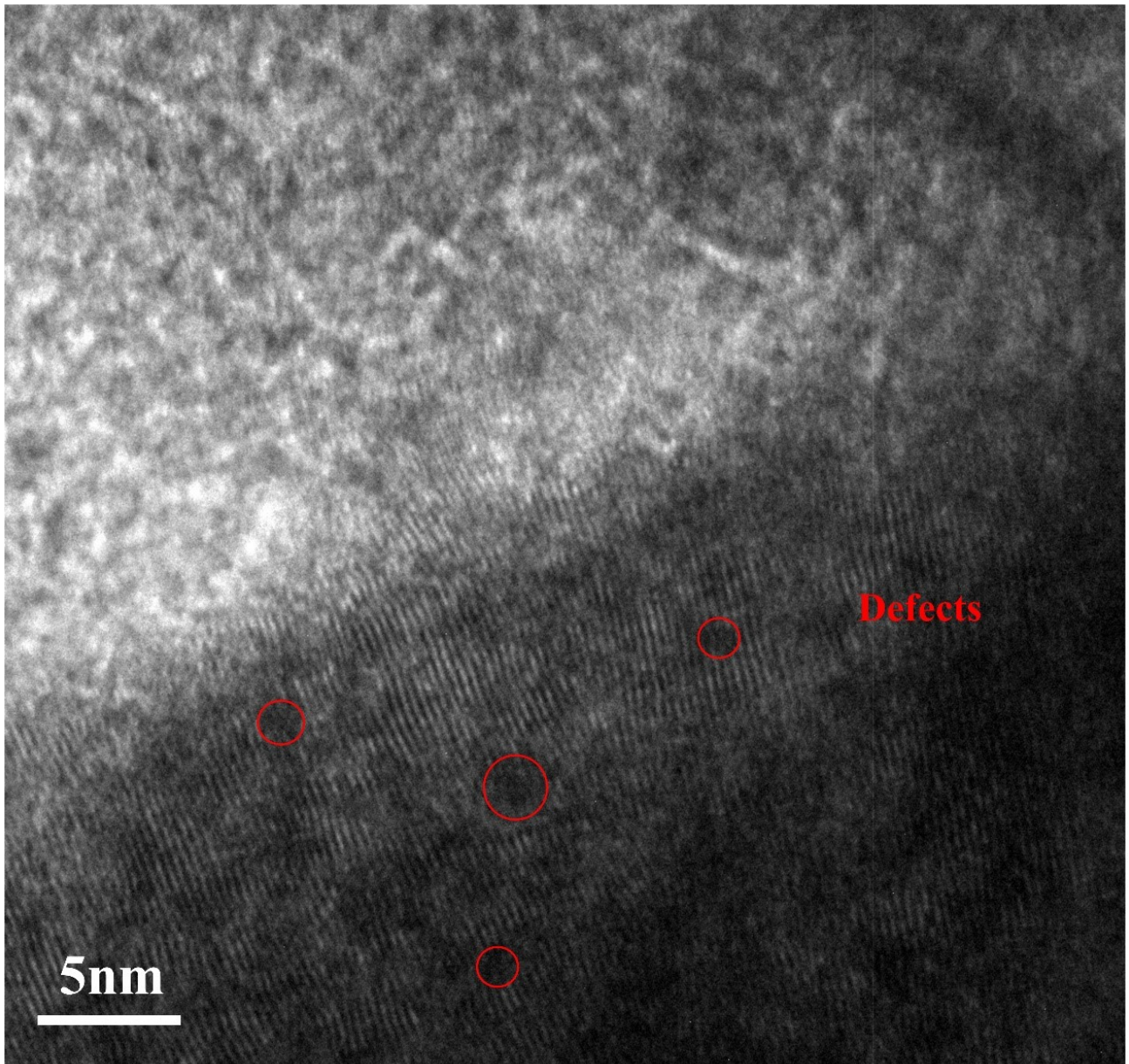


Figure S 3. HRTEM image of CoB/CeO<sub>2</sub> at 5 nm.

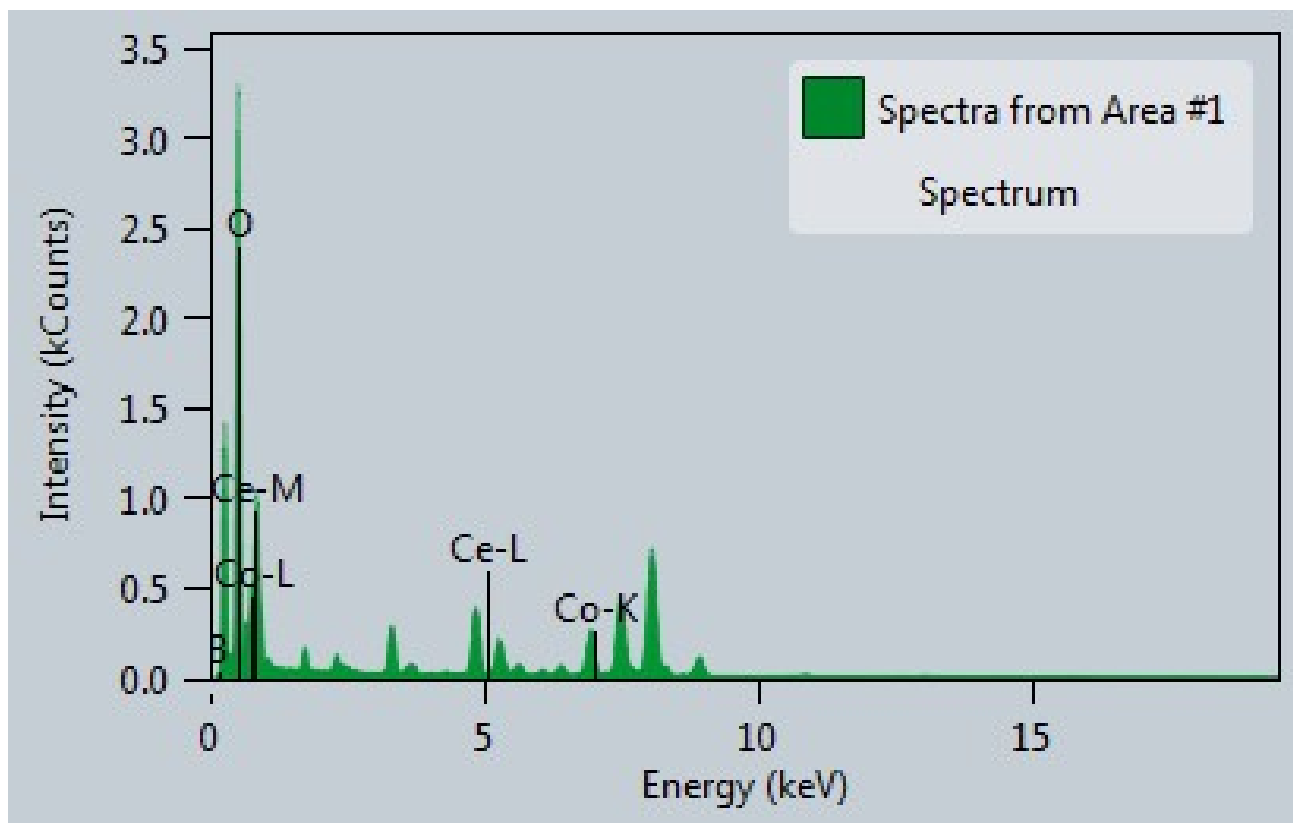


Figure S 4. EDX spectrum of CoB/CeO<sub>2</sub>.

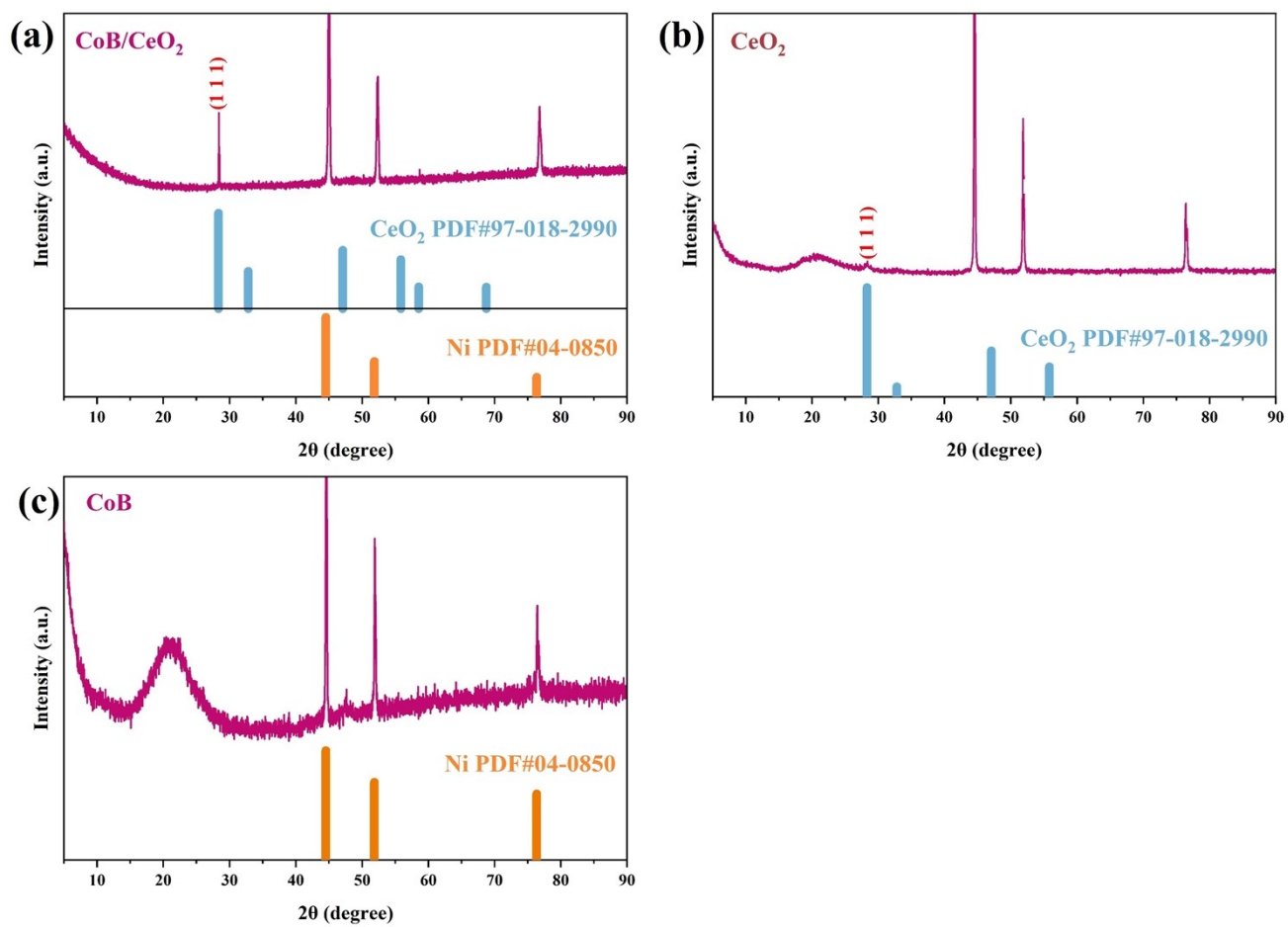


Figure S 5. XRD patterns of CoB/CeO<sub>2</sub>, CeO<sub>2</sub>, and CoB.



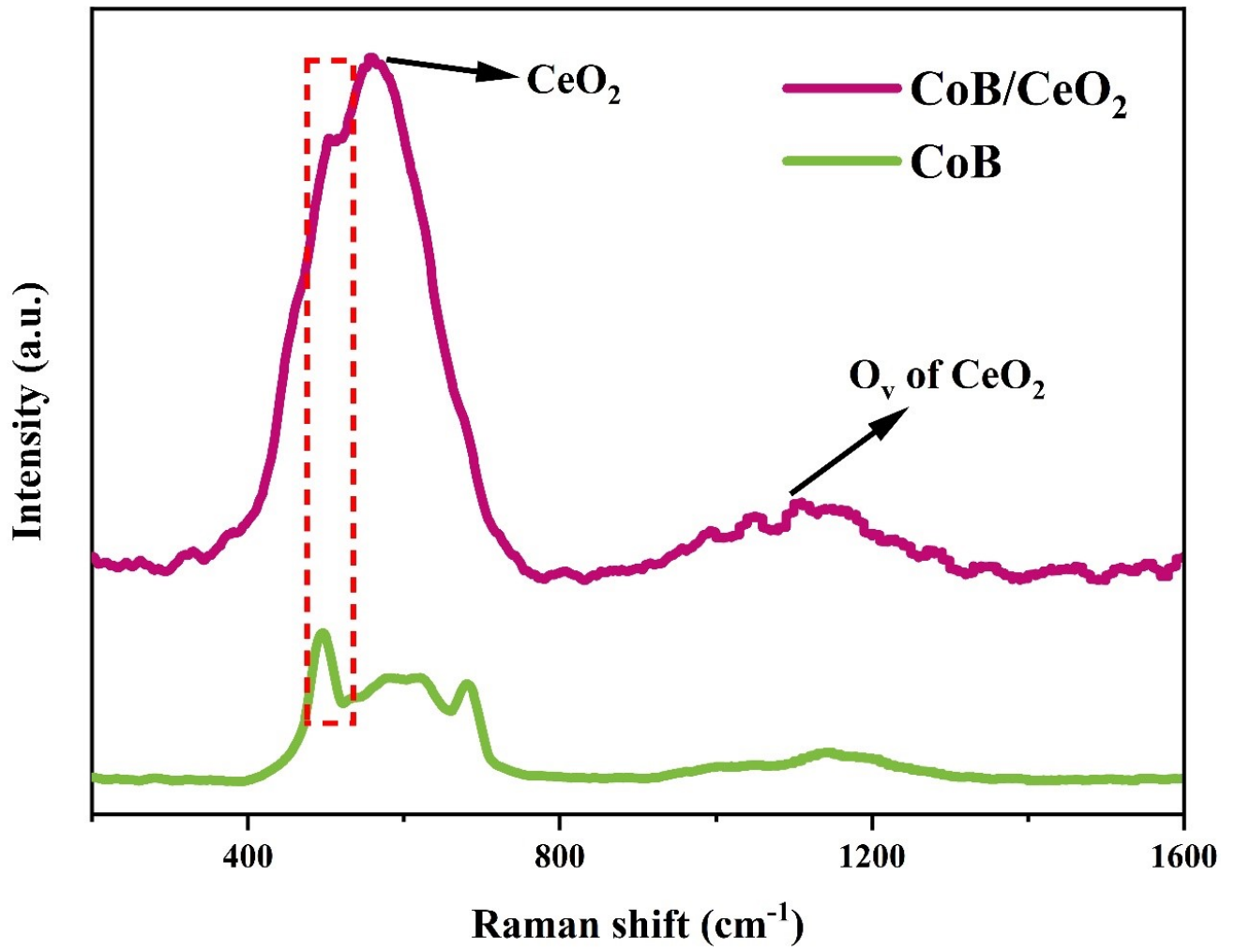


Figure S 6. Raman spectra of CoB and CoB/CeO<sub>2</sub>.

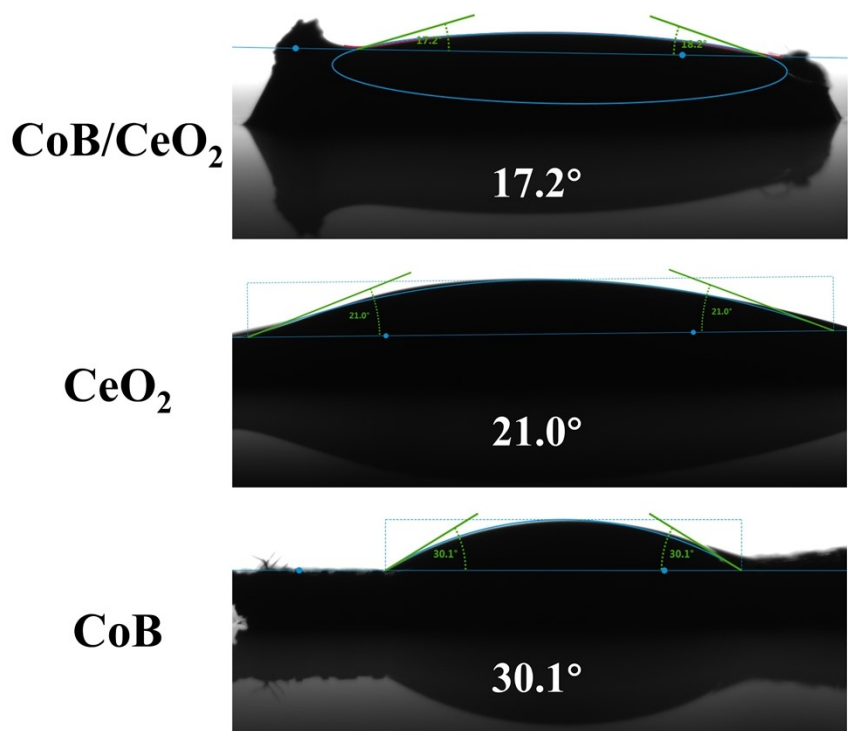


Figure S 7. The water contact angles of CoB/CeO<sub>2</sub>, CeO<sub>2</sub>, and CoB.



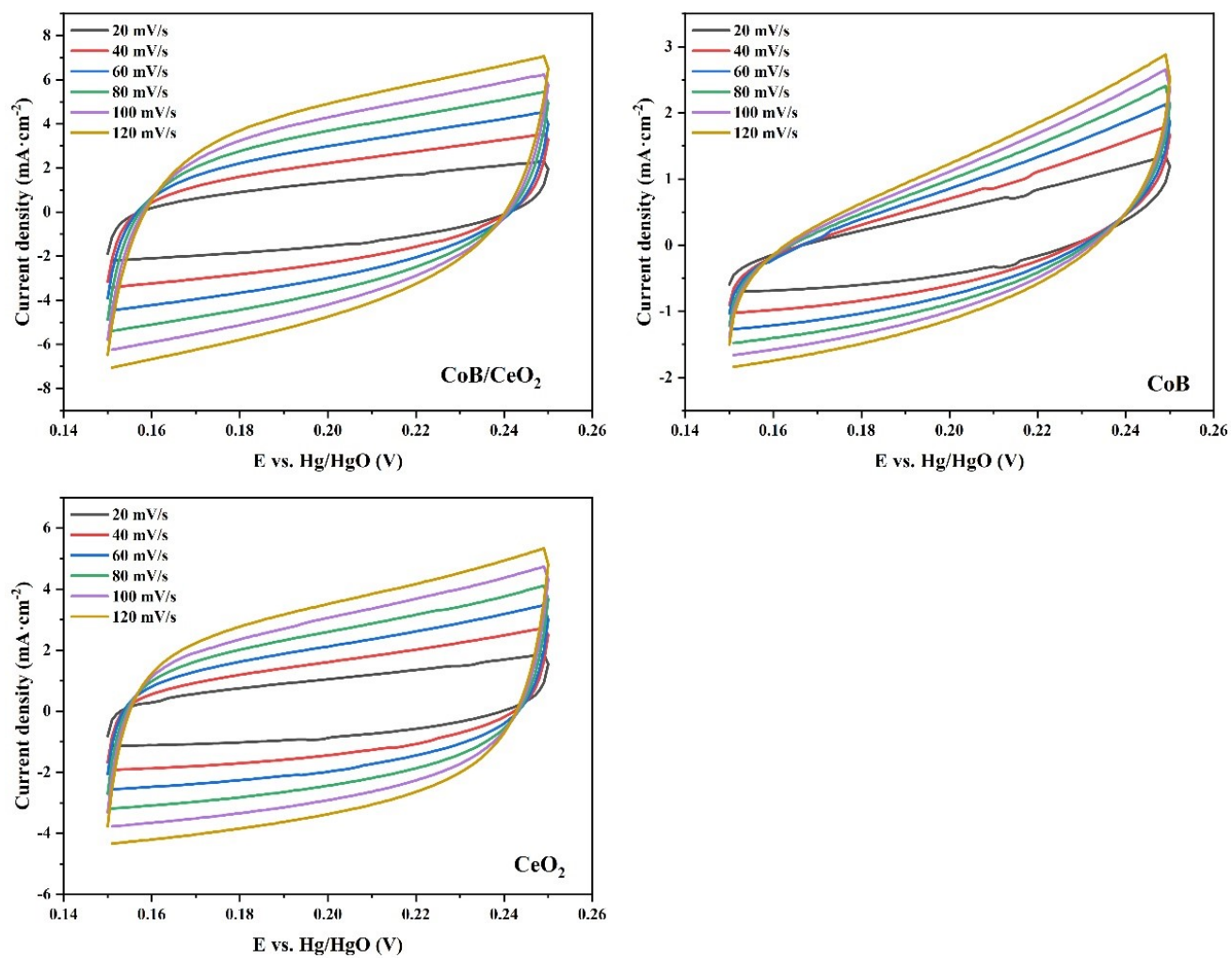


Figure S 8. CV curves of CoB/CeO<sub>2</sub>, CoB, and CeO<sub>2</sub> in 1.0 M KOH.

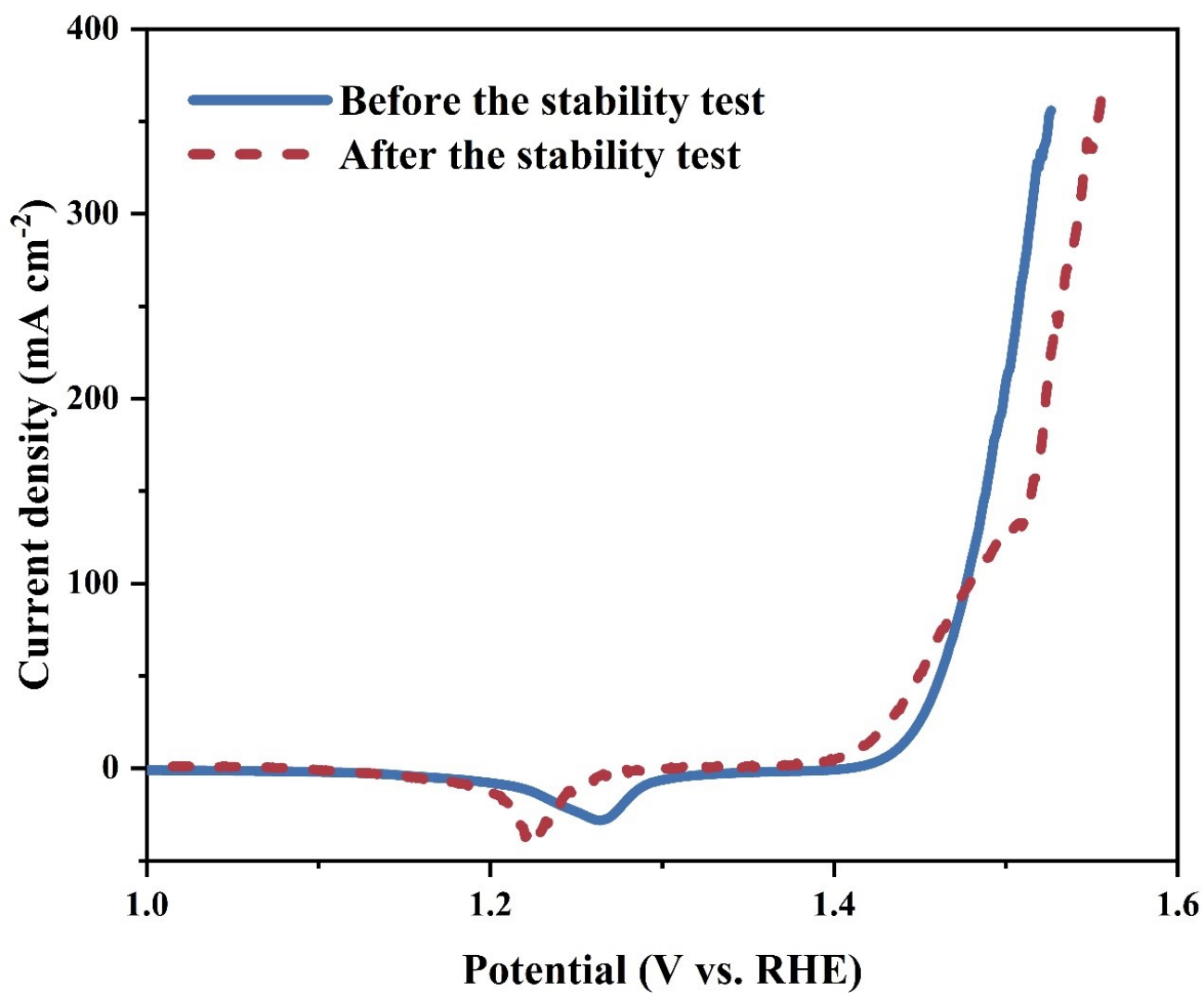


Figure S 9. LSV curves of CoB/CeO<sub>2</sub> in 1.0 M KOH before and after stability testing.

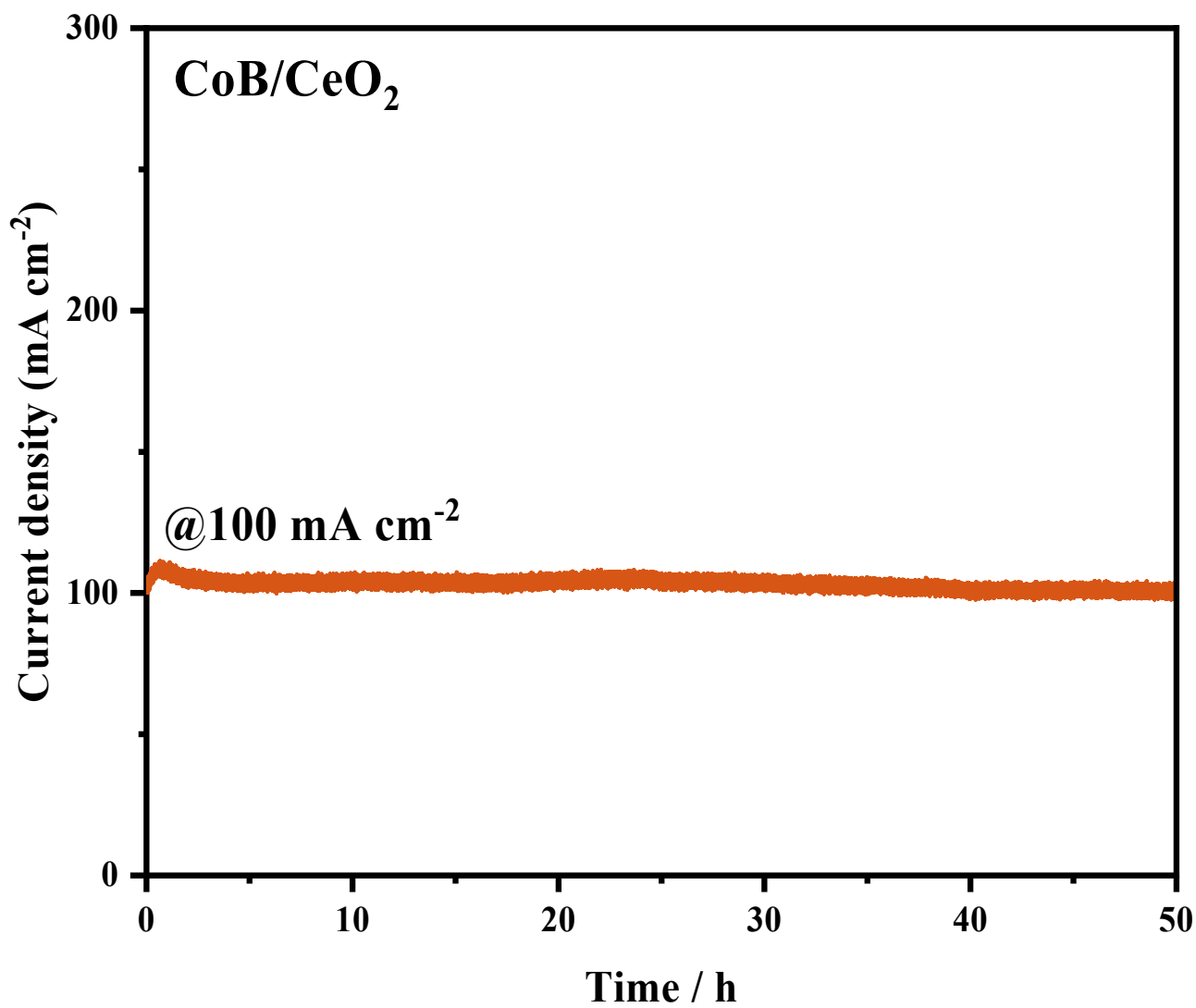


Figure S 10. I-T durability test of CoB/CeO<sub>2</sub> at 100 mA cm<sup>-2</sup> for 50 hours.

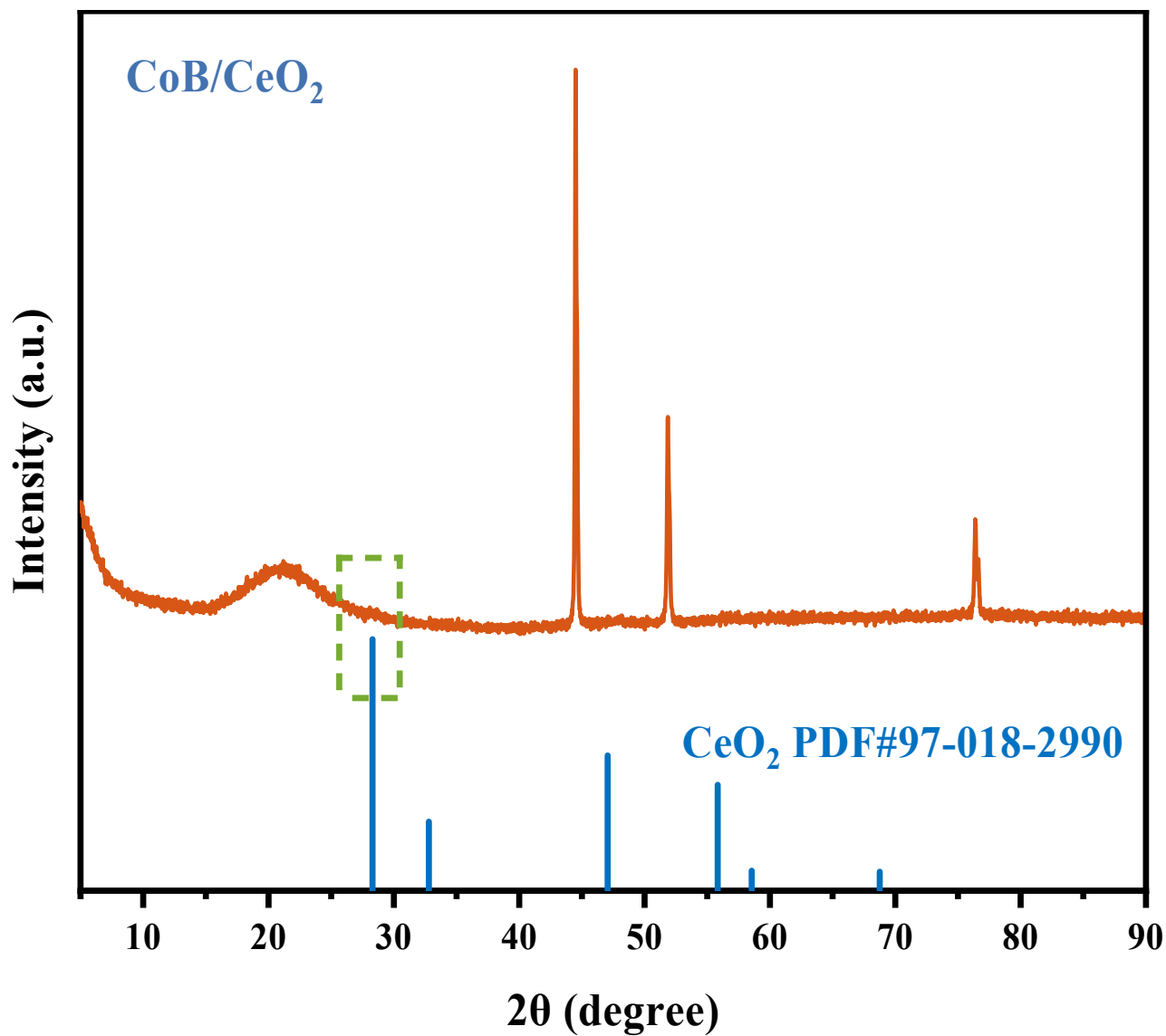


Figure S 11. XRD pattern of CoB/CeO<sub>2</sub> after 50 hours of stability testing in 1.0 M KOH.

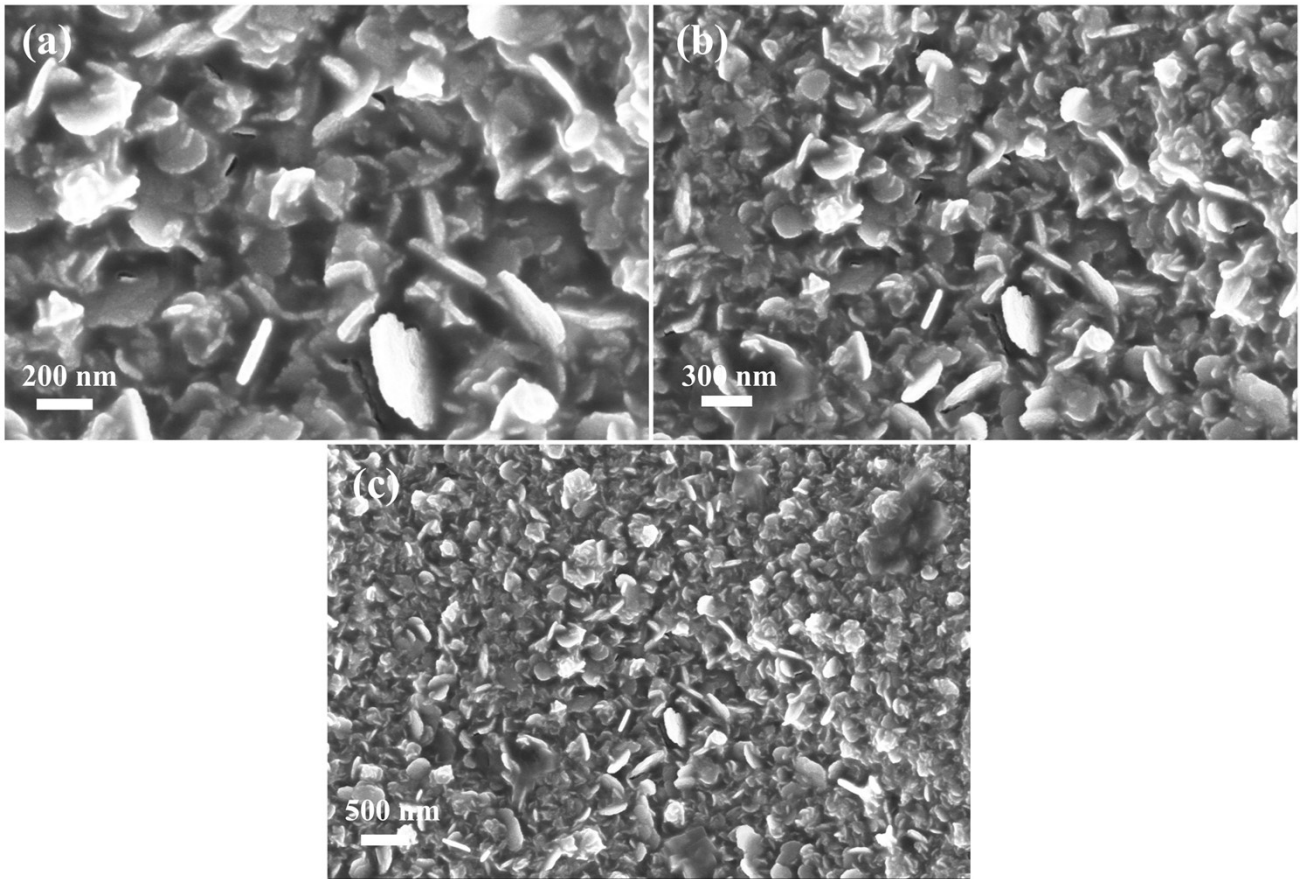


Figure S 12. SEM images of CoB/CeO<sub>2</sub> after 50 hours of stability testing in 1.0 M KOH at (a) 200 nm, (b) 300 nm, and (c) 500 nm.

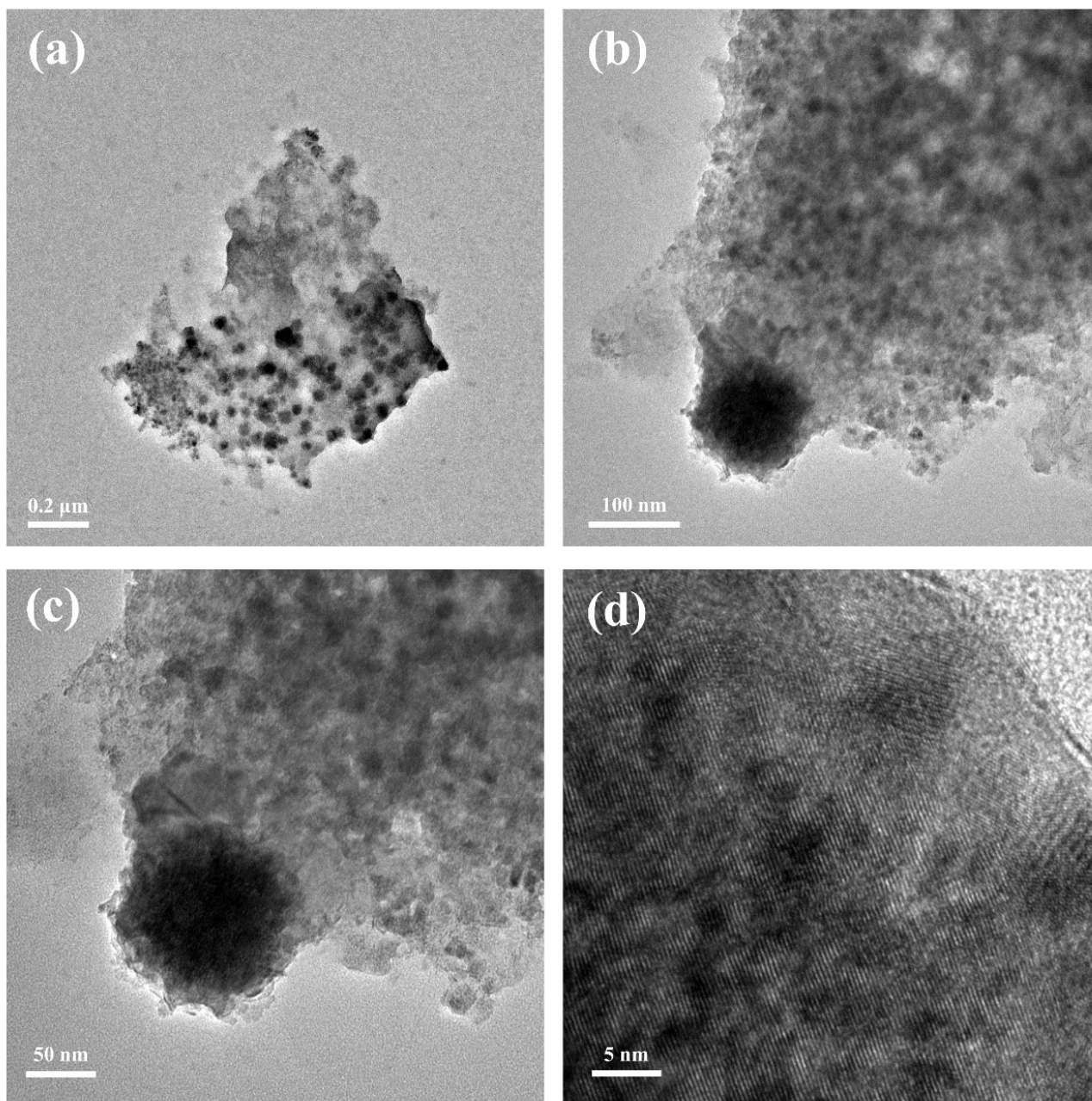


Figure S 13. After 50 hours of stability testing in 1.0 M KOH, TEM images of CoB/CeO<sub>2</sub> at (a) 0.2 μm, (b) 100 nm, and (c) 50 nm scales, and (d) HRTEM image at 5 nm scale.

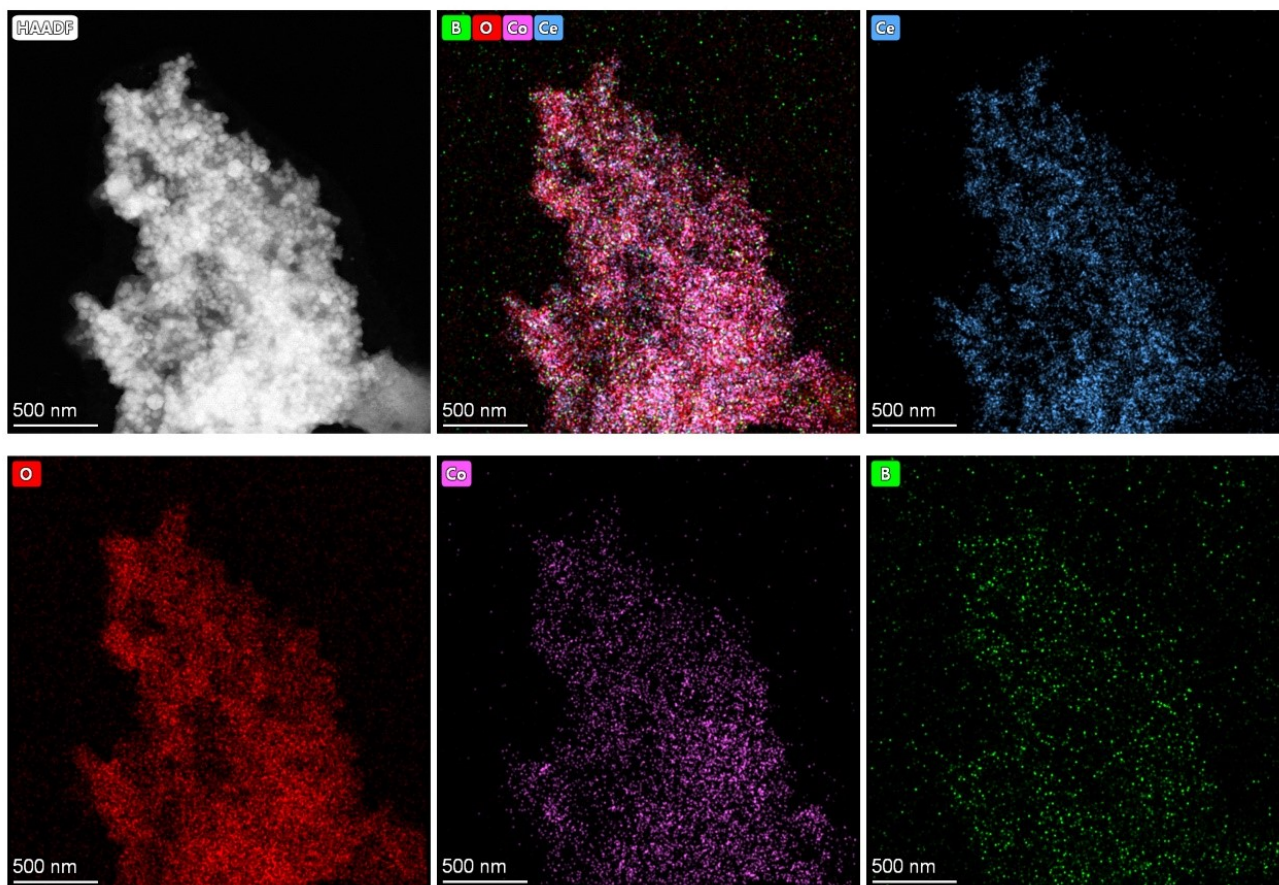


Figure S 14. Elemental mapping image of CoB/CeO<sub>2</sub> after 50 hours of stability testing in 1.0 M KOH.



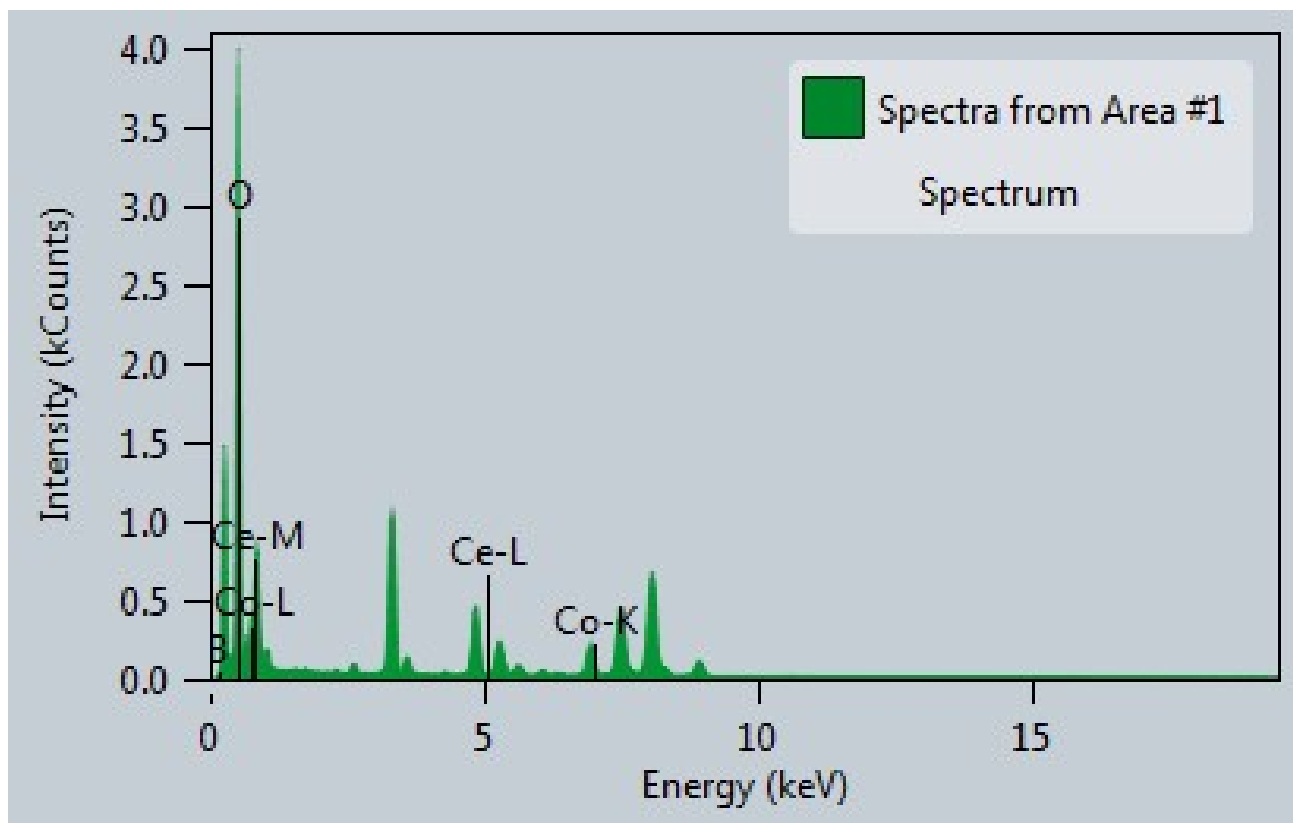


Figure S 15. EDX spectrum of CoB/CeO<sub>2</sub> after 50 hours of stability testing in 1.0 M KOH.

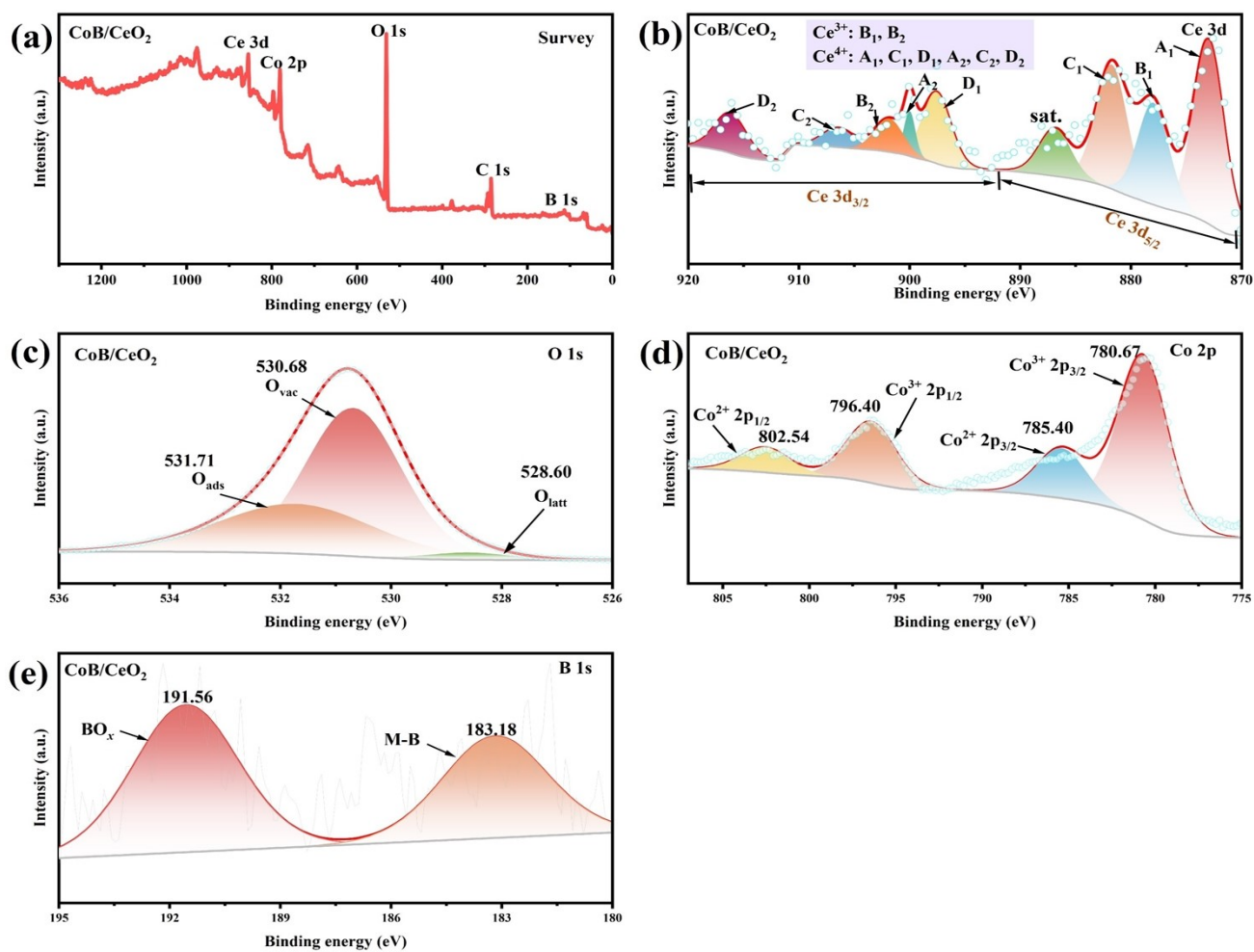


Figure S 16. XPS spectra of CoB/CeO<sub>2</sub> after 50 hours of stability testing in 1.0 M KOH: (a) Survey spectrum, (b) Ce 3d spectrum, (c) O 1s spectrum, (d) Co 2p spectrum, and (e) B 1s spectrum.

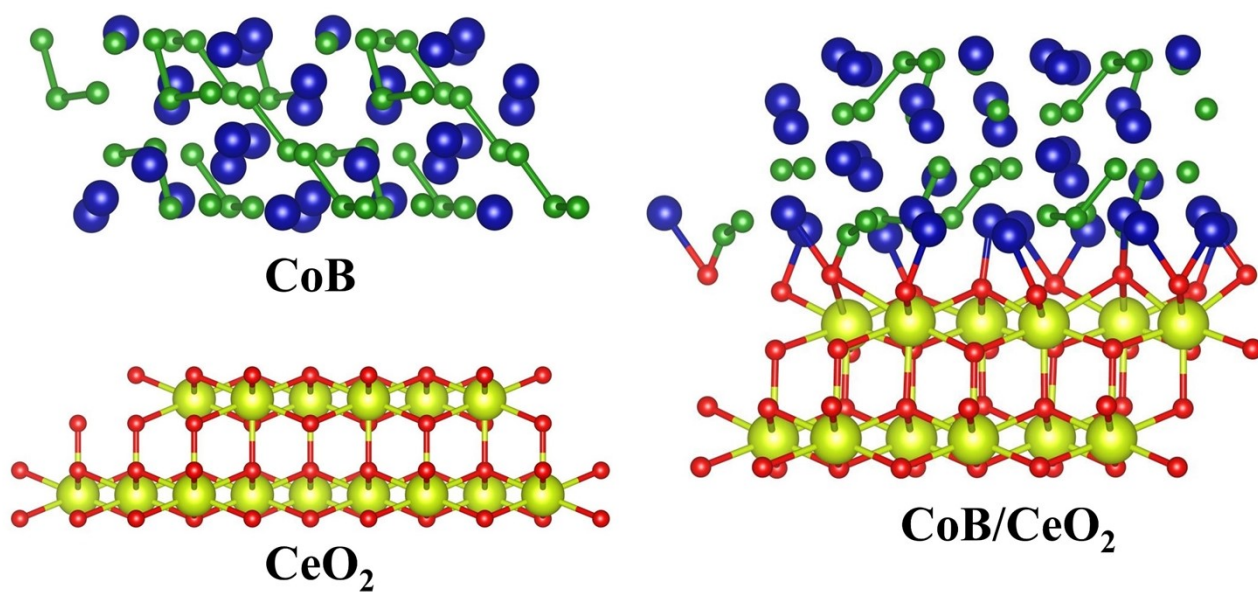


Figure S 17. Optimized atomic models of CoB, CeO<sub>2</sub>, and CoB/CeO<sub>2</sub>.

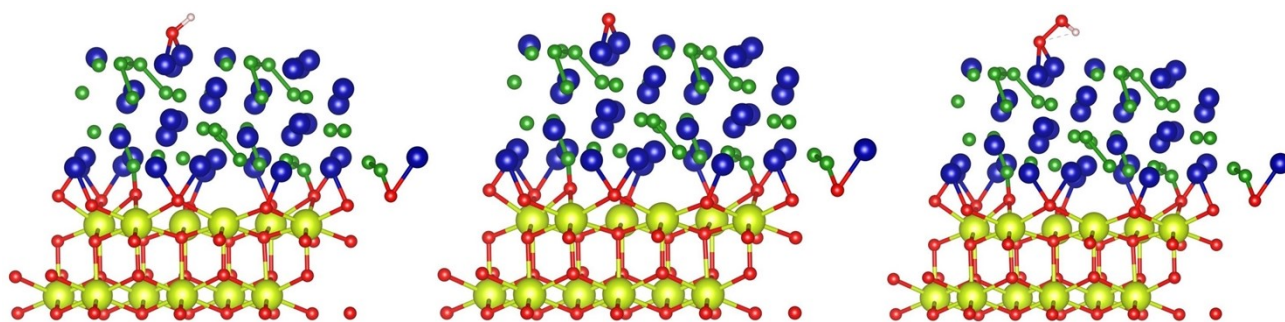


Figure S 18. The model of CoB/CeO<sub>2</sub> catalyst with oxygen vacancies after the adsorption of OH, O, and OOH.

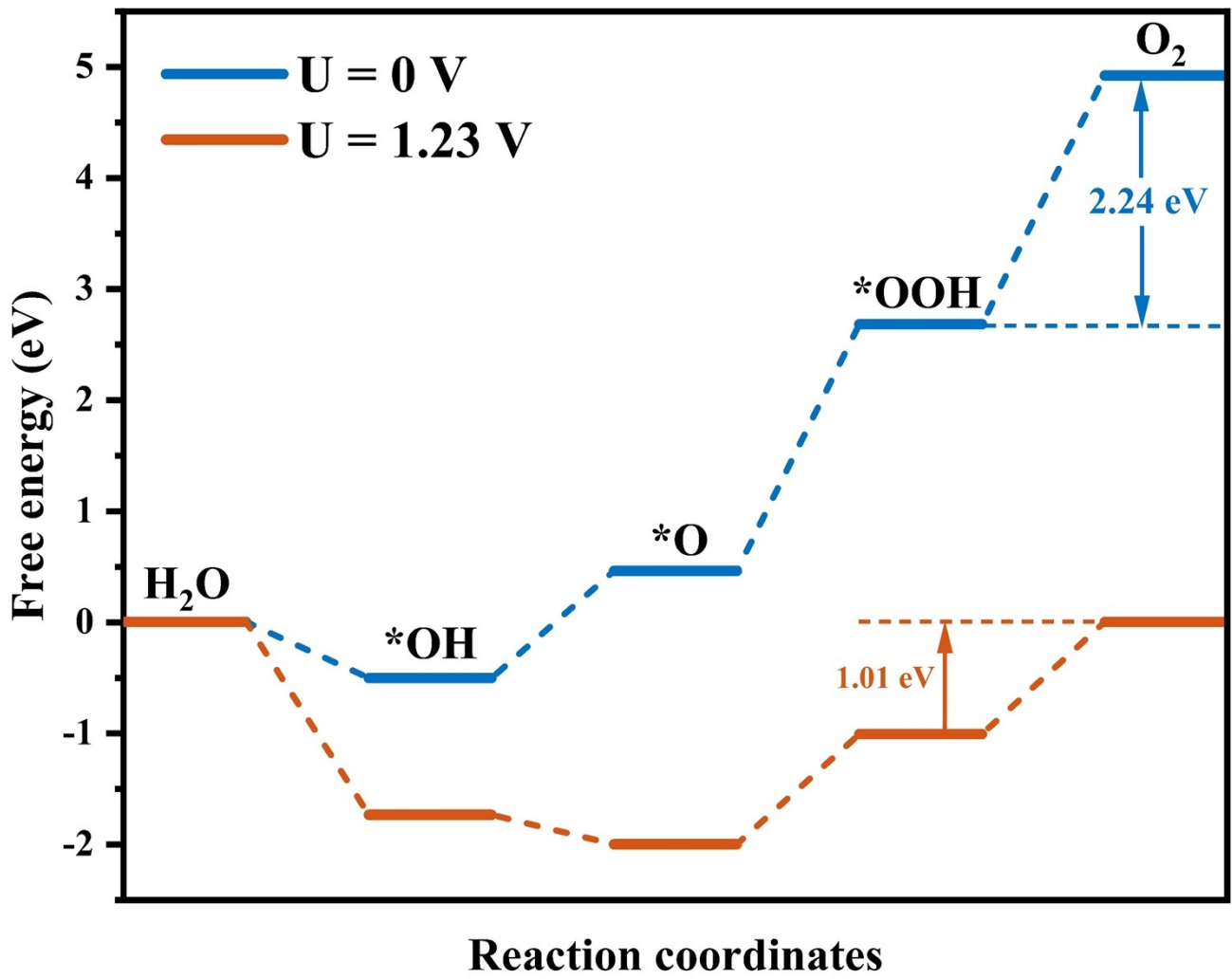


Figure S 19. The free energy distribution of oxygen vacancies on CoB/CeO<sub>2</sub> at U=0 V and U=1.23 V.

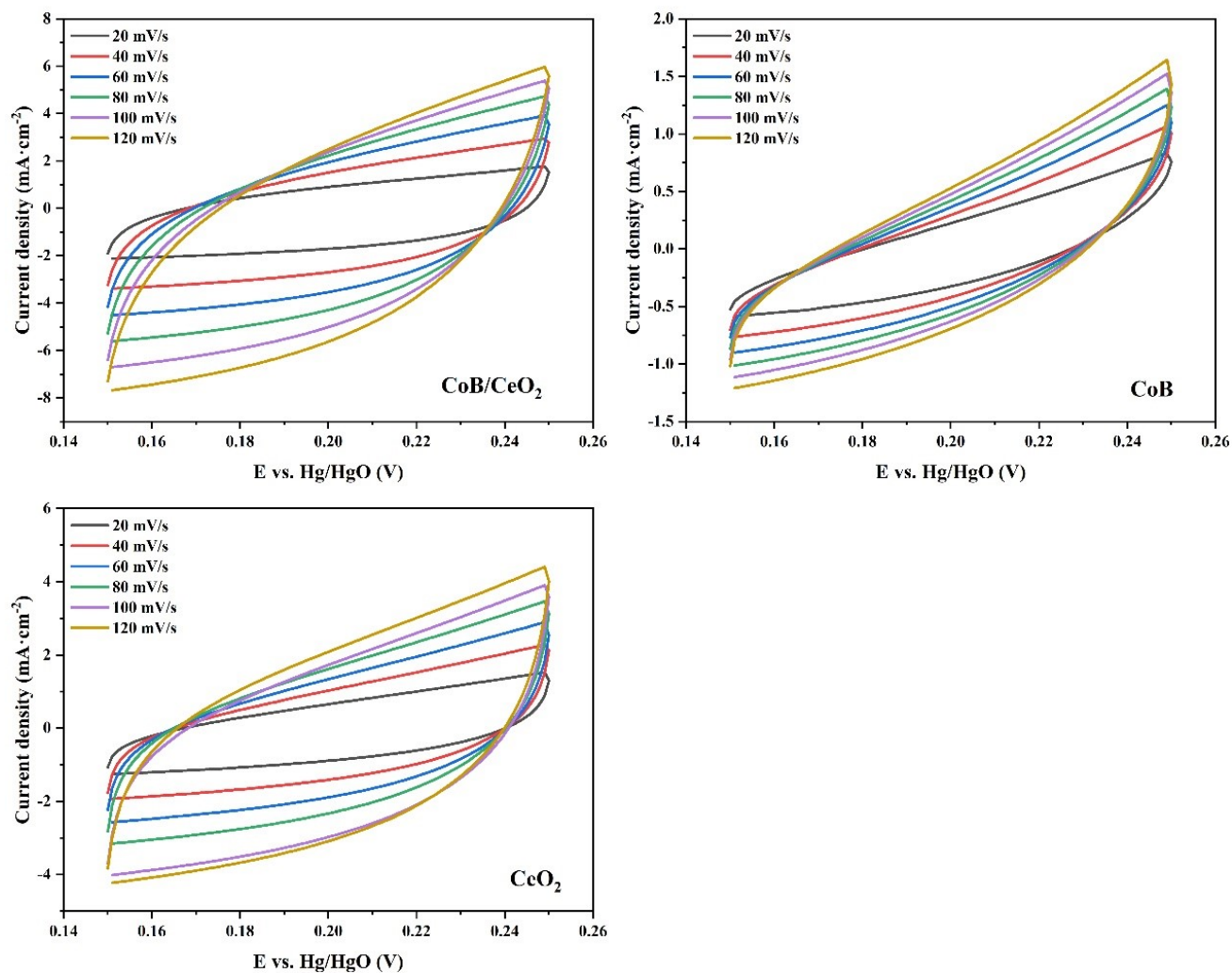


Figure S 20. CV curves of CoB/CeO<sub>2</sub>, CoB, and CeO<sub>2</sub> in simulated seawater (1.0 M KOH + 0.5 M NaCl).

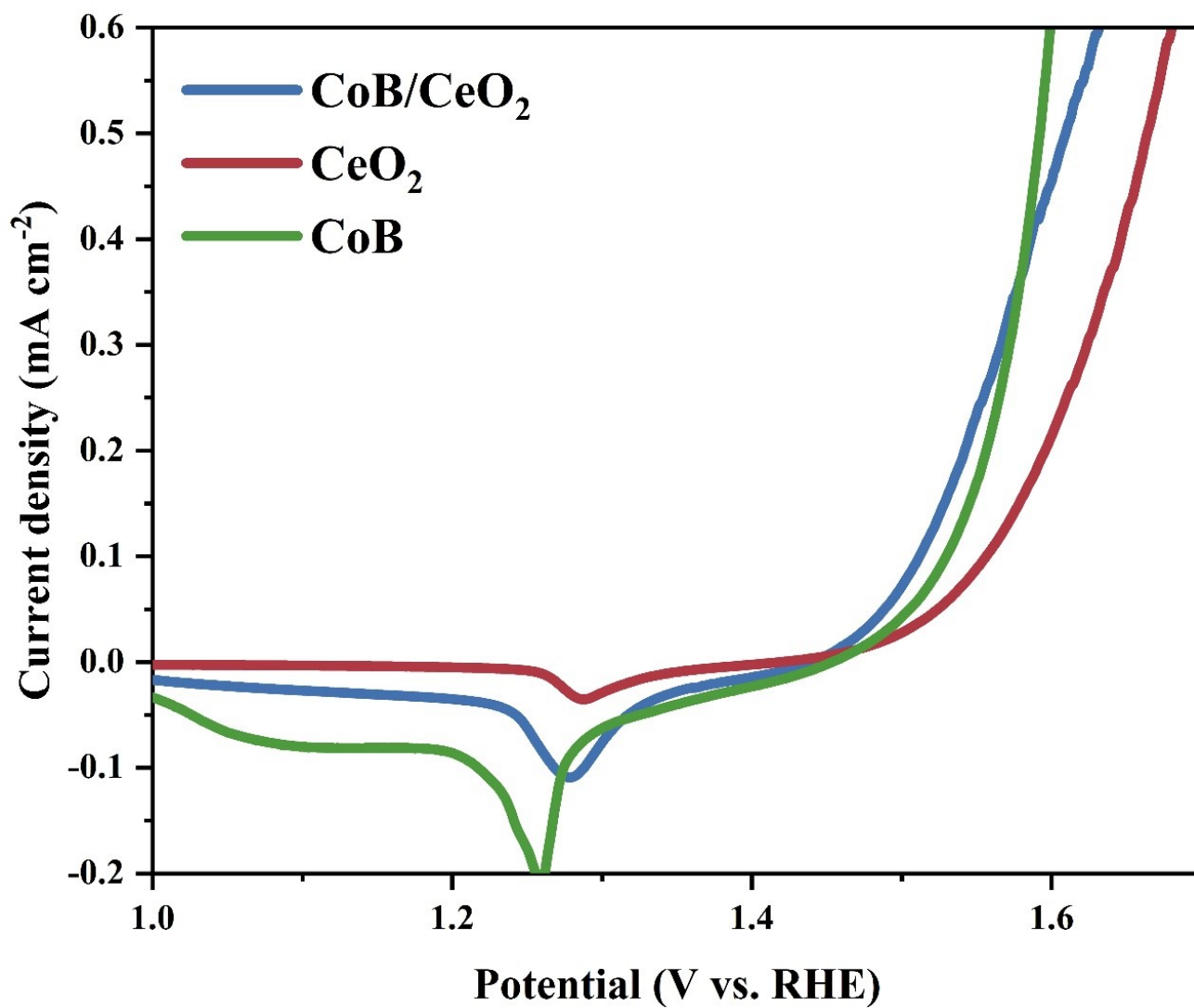


Figure S 21. Normalized LSV curves of CoB/CeO<sub>2</sub>, CoB, and CeO<sub>2</sub> in simulated seawater (1.0 M KOH + 0.5 M NaCl).

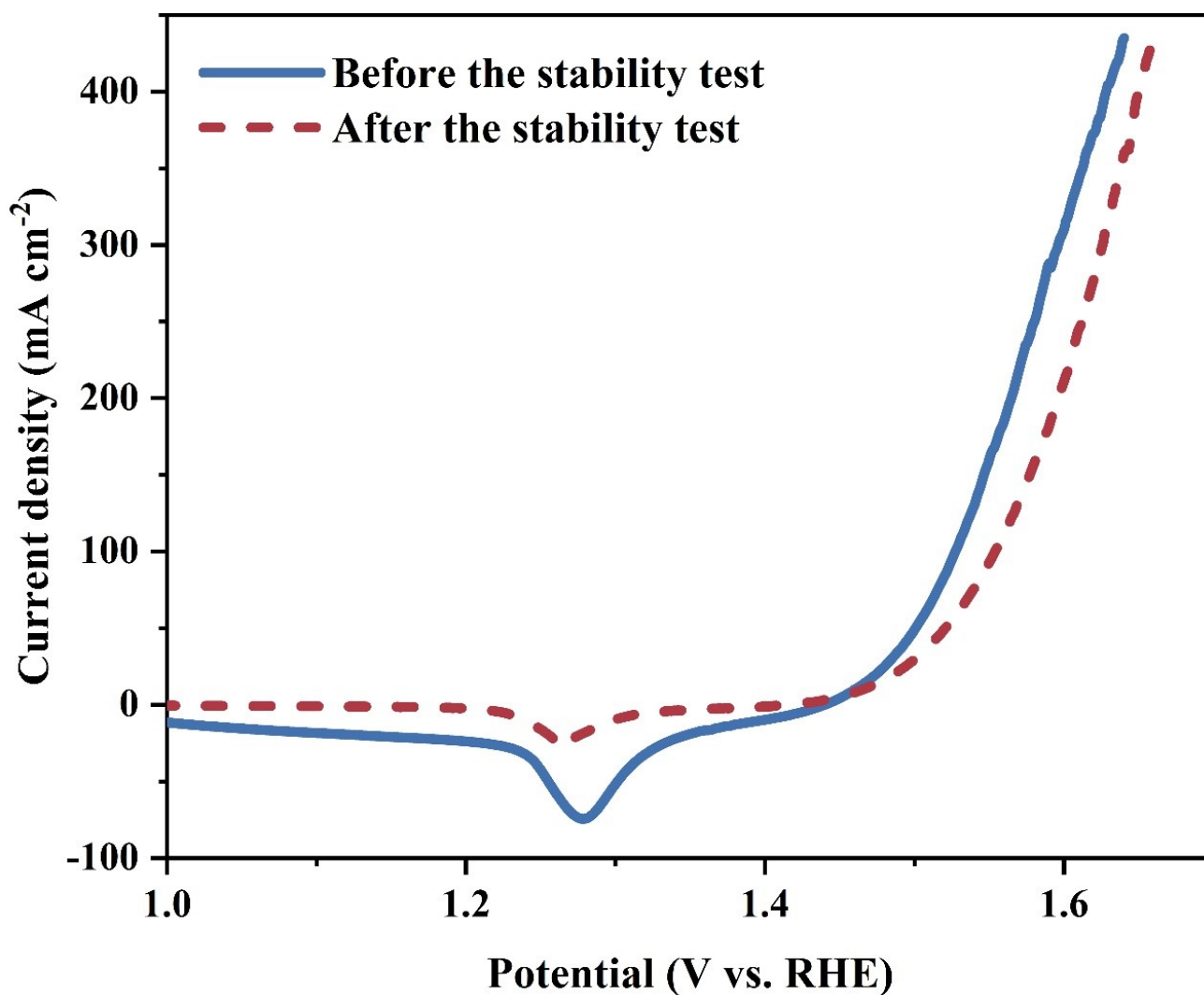


Figure S 22. LSV curves of CoB/CeO<sub>2</sub> in simulated seawater (1.0 M KOH + 0.5 M NaCl) before and after stability testing.

Table S 1. ECSA values of CoB/CeO<sub>2</sub>, CeO<sub>2</sub> and CoB in 1.0 M KOH.

Catalysts	ECSA
CoB/CeO <sub>2</sub>	840.50
CeO <sub>2</sub>	615.75
CoB	171.50

Table S 2. Comparison of OER activity at 1.0 M KOH and 10 mA cm<sup>-2</sup> current density.

Catalyst	At 10 mA cm <sup>-2</sup>	Ref.
CoB/CeO <sub>2</sub>	207	This work



Co <sub>3</sub> S <sub>4</sub> /CeO <sub>2</sub> -CF	213	1
N-CoP/CeO <sub>2</sub>	215	2
CeO <sub>2-x</sub> /NiFe-LDH	216	3
CeO <sub>2</sub> @Co <sub>2</sub> N	219	4
V-CoP@a-CeO <sub>2</sub>	225	5
Co <sub>4</sub> N-CeO <sub>2</sub> /GP	239	6
Fe <sub>2</sub> P-CoP/CeO <sub>2</sub> -20	248	7
Ce/N-NiO	250	8
CeO <sub>2</sub> -Ni <sub>3</sub> S <sub>2</sub> /NF	251	9
CeO <sub>2</sub> -NiCoP <sub>x</sub> /NCF	260	10
NF/Co <sub>4</sub> N@CeO <sub>2</sub>	263	11
CeO <sub>2</sub> -CuCoO/NF	266	12
MnCo <sub>2</sub> O <sub>4</sub> /CeO <sub>2</sub>	276	13
Co-Fe-B	280	14
CeFeCe0.5	329	15

Table S 3. Comparison of OER activity at 1.0 M KOH and 100 mA cm<sup>-2</sup> current density.

Catalyst	At 100 mA cm <sup>-2</sup>	Ref.
CoB/CeO <sub>2</sub>	247	This work
Co/CeO <sub>2</sub> @CF	282	16
CoP/CeO <sub>2</sub> -FeO <sub>x</sub> H	285	17
Co <sub>3</sub> O <sub>4</sub> -CeO <sub>2</sub> @FNF	290	18
CeO <sub>2</sub> -Co(OH) <sub>2</sub>	299	19
Co <sub>4</sub> N-CeO <sub>2</sub> /GP	320	6
CeO <sub>2</sub> /CoS <sub>1.97</sub>	320	20
NF/Co <sub>4</sub> N@CeO <sub>2</sub>	325	11
CoO-CeO <sub>2</sub>	340	21
V-CoP@a-CeO <sub>2</sub>	340	5
Co <sub>0.4</sub> Ni <sub>1.6</sub> P-CeO <sub>2</sub>	343	22
CeO <sub>2</sub> @Co <sub>2</sub> N	345	4
CeO <sub>2</sub> /Co <sub>3</sub> O <sub>4</sub>	350	23
Co <sub>3</sub> S <sub>4</sub> /CeO <sub>2</sub> -CF	355	1
CeO <sub>2</sub> -Ni <sub>3</sub> S <sub>2</sub> /NF	364	9

3DOM-Co <sub>3</sub> O <sub>4</sub> /CeO <sub>2</sub>	370	24
CeO <sub>2</sub> -CuCoO/NF	490	12

Table S 4. ECSA values of CoB/CeO<sub>2</sub>, CeO<sub>2</sub> and CoB in simulated seawater (1.0 M KOH + 0.5 M NaCl).

Catalysts	ECSA
CoB/CeO <sub>2</sub>	681.25
CeO <sub>2</sub>	457.75
CoB	83.00

Table S 5. Comparison of OER activity in simulated seawater (1.0 M KOH + 0.5 M NaCl) and 10 mA cm<sup>-2</sup> current density.

Catalyst	At 10 mA cm <sup>-2</sup>	Ref.
CoB/CeO <sub>2</sub>	230	This work
CeO <sub>x</sub> @NiCo <sub>2</sub> O <sub>4</sub> /NF	240	25
Fe <sub>2</sub> P/NiCoP	255	26
NF@NiB <sub>x</sub> -3h	261	27
Co <sub>8</sub> FeS <sub>8</sub> /ESM-900	271	28
CoNiWFeVO <sub>x</sub>	272	29
MoC-Mo <sub>2</sub> C/CNTs	279	30
Ce-NiSe <sub>2</sub> /CoP	304	31
Co-B	305	32
NiCo <sub>2</sub> O <sub>4</sub> /NiCoP	340	33
CSC-Fe	359	34
NiMoSe@CC	360	35
NiMn/Ti-1	386	36

## References

1. Z. Feng, J. Pu, M. Liu, W. Zhang, X. Zhang, L. Cui and J. Liu, Facile construction of hierarchical Co(3)S(4)/CeO(2) heterogeneous nanorod array on cobalt foam for electrocatalytic overall water splitting, *J Colloid Interface Sci*, 2022, **613**, 806-813.
2. L. Zhang, Y. Lei, W. Xu, D. Wang, Y. Zhao, W. Chen, X. Xiang, X. Pang, B. Zhang and H. Shang, Highly active and durable nitrogen-doped CoP/CeO<sub>2</sub> nanowire heterostructures for overall water splitting, *Chemical Engineering Journal*, 2023, **460**.

3. Y. Du, D. Liu, T. Li, Y. Yan, Y. Liang, S. Yan and Z. Zou, A phase transformation-free redox couple mediated electrocatalytic oxygen evolution reaction, *Applied Catalysis B: Environmental*, 2022, **306**.
4. J. Zhang, W. He, H. B. Aiyappa, T. Quast, S. Dieckhöfer, D. Öhl, J. R. C. Junqueira, Y. T. Chen, J. Masa and W. Schuhmann, Hollow CeO<sub>2</sub>@Co<sub>2</sub>N Nanosheets Derived from Co-ZIF-L for Boosting the Oxygen Evolution Reaction, *Advanced Materials Interfaces*, 2021, **8**.
5. L. Yang, R. Liu and L. Jiao, Electronic Redistribution: Construction and Modulation of Interface Engineering on CoP for Enhancing Overall Water Splitting, *Advanced Functional Materials*, 2020, **30**.
6. H. Sun, C. Tian, G. Fan, J. Qi, Z. Liu, Z. Yan, F. Cheng, J. Chen, C. P. Li and M. Du, Boosting Activity on Co<sub>4</sub>N Porous Nanosheet by Coupling CeO<sub>2</sub> for Efficient Electrochemical Overall Water Splitting at High Current Densities, *Advanced Functional Materials*, 2020, **30**.
7. X. Ding, J. Yu, W. Huang, D. Chen, W. Lin and Z. Xie, Modulation of the interfacial charge density on Fe<sub>2</sub>P–CoP by coupling CeO<sub>2</sub> for accelerating alkaline electrocatalytic hydrogen evolution reaction and overall water splitting, *Chemical Engineering Journal*, 2023, **451**.
8. F. Yang, X. Zhang, L. Zhou, S. Lin, X. Cao, J. Jiang and X. Lu, Tuning the interfacial electronic coupling of NiO via CeO<sub>2</sub> and nitrogen co-decoration for highly efficient oxygen evolution reaction, *Chemical Engineering Journal*, 2022, **432**.
9. Z. Huang, X. Liao, W. Zhang, J. Hu and Q. Gao, Ceria-Promoted Reconstruction of Ni-Based Electrocatalysts toward Efficient Oxygen Evolution, *ACS Catalysis*, 2022, **12**, 13951-13960.
10. S. Wen, J. Huang, T. Li, W. Chen, G. Chen, Q. Zhang, X. Zhang, Q. Qian and K. Ostrikov, Multiphase nanosheet-nanowire cerium oxide and nickel-cobalt phosphide for highly-efficient electrocatalytic overall water splitting, *Applied Catalysis B: Environmental*, 2022, **316**.
11. P. Zhou, G. Hai, G. Zhao, R. Li, X. Huang, Y. Lu and G. Wang, CeO<sub>2</sub> as an “electron pump” to boost the performance of Co<sub>4</sub>N in electrocatalytic hydrogen evolution, oxygen evolution and biomass oxidation valorization, *Applied Catalysis B: Environmental*, 2023, **325**.
12. L. Li, L. Cao, Q. He, B. Shang, J. Chen, J. Lei, N. Li and F. Pan, A novel strategy to simultaneously tailor morphology and electronic structure of CuCo hybrid oxides for enhanced electrocatalytic performance in overall water splitting, *Sustainable Energy & Fuels*, 2020, **4**, 2775-2781.
13. C. Fan, X. Wu, M. Li, X. Wang, Y. Zhu, G. Fu, T. Ma and Y. Tang, Surface chemical reconstruction of hierarchical hollow inverse-spinel manganese cobalt oxide boosting oxygen evolution reaction, *Chemical Engineering Journal*, 2022, **431**.
14. C. Qiang, L. Zhang, H. He, Y. Liu, Y. Zhao, T. Sheng, S. Liu, X. Wu and Z. Fang, Efficient electrocatalytic water splitting by bimetallic cobalt iron boride nanoparticles with controlled electronic structure, *Journal of Colloid and Interface Science*, 2021, **604**, 650-659.
15. Y. S. Park, F. Liu, D. Diercks, D. Braaten, B. Liu and C. Duan, High-performance anion exchange membrane water electrolyzer enabled by highly active oxygen evolution reaction electrocatalysts: Synergistic effect of doping and heterostructure, *Applied Catalysis B: Environmental*, 2022, **318**.
16. H. Chen, H. B. Huang, H. H. Li, S. Z. Zhao, L. D. Wang, J. Zhang, S. L. Zhong, C. F. Lao, L. M. Cao and C. T. He, Self-Supporting Co/CeO<sub>2</sub> Heterostructures for Ampere-Level Current Density Alkaline Water Electrolysis, *Inorg Chem*, 2023, **62**, 3297-3304.
17. Y. Tan, Q. Che and Q. Li, Constructing Double-Layer CoP/CeO<sub>2</sub>–FeOxH Hybrid Catalysts for Alkaline and Neutral Water Splitting, *ACS Sustainable Chemistry & Engineering*, 2021, **9**, 11981-11990.
18. M. Liu, T. Chen, W. Zhang, S. Wei, Y. Cheng and J. Liu, In situ construction of pollen-petal-like heterostructured Co<sub>3</sub>O<sub>4</sub>–CeO<sub>2</sub> on 3D FeNi<sub>3</sub> foam as a bifunctional catalyst for overall water splitting, *Sustainable Energy & Fuels*, 2021, **5**, 2181-2189.

19. M. Chen, Y. Lv, P. Wu, L. Dong, X. He and L. Cui, The electron engineering of CeO<sub>2</sub>/Co(OH)<sub>2</sub> hybrids to enhance the performance for overall water splitting in alkaline media, *Journal of Electroanalytical Chemistry*, 2022, **918**.
20. T. Dai, X. Zhang, M. Sun, B. Huang, N. Zhang, P. Da, R. Yang, Z. He, W. Wang, P. Xi and C. H. Yan, Uncovering the Promotion of CeO(2) /CoS(1.97) Heterostructure with Specific Spatial Architectures on Oxygen Evolution Reaction, *Adv Mater*, 2021, **33**, e2102593.
21. X. Ren, F. Hou, F. Wang, X. Zhang and Q. Wang, Porous CoO-CeO<sub>2</sub> heterostructures as highly active and stable electrocatalysts for water oxidation, *International Journal of Hydrogen Energy*, 2018, **43**, 22529-22537.
22. Y. Cong, X. Chen, Y. Mei, J. Ye and T. T. Li, CeO(2) decorated bimetallic phosphide nanowire arrays for enhanced oxygen evolution reaction electrocatalysis via interface engineering, *Dalton Trans*, 2022, **51**, 2923-2931.
23. X. Yang, Z. Tao, Y. Wu, W. Lin and J. Zheng, Electrochemical deposition of CeO<sub>2</sub> nanocrystals on Co<sub>3</sub>O<sub>4</sub> nanoneedle arrays for efficient oxygen evolution, *Journal of Alloys and Compounds*, 2020, **828**.
24. X. Wang, M. Liu, H. Yu, H. Zhang, S. Yan, C. Zhang and S. Liu, Oxygen-deficient 3D-ordered multistage porous interfacial catalysts with enhanced water oxidation performance, *Journal of Materials Chemistry A*, 2020, **8**, 22886-22892.
25. W. Liu, J. Zhao, L. Dai, Y. Qi, K. Liang, J. Bao and Y. Ren, Interface Engineering Overall Seawater Splitting of Self-Supporting CeO(x)@NiCo(2)O(4) Arrays, *Inorg Chem*, 2024, **63**, 6016-6025.
26. H. Xu, L. Jin, K. Wang, L. Yang, Y. Liu, G. He and H. Chen, Interfacial built-in electric fields facilitating surface reconstruction in heterojunction electrocatalysts for boosting water oxidation and simulated seawater oxidation, *Fuel*, 2024, **369**.
27. Z. Lu, R. Liang, Y. Shao and W. Hao, Mild and Fast Construction of Ni-Based Electrodes for Industrial-Grade Water Splitting, *Inorganics*, 2023, **11**.
28. L. Cui, L. Zhang and Y. Shen, Eggshell membrane-derived metal sulfide catalysts for seawater splitting, *Green Chemistry*, 2024, **26**, 7879-7890.
29. Y. Li, Y. Li, R. Wang, C. Xia, H. Li, L. Cao and B. Dong, Ultrathin fan-like multimetallic oxide as a superior oxygen evolution electrocatalyst in alkaline water and seawater, *International Journal of Hydrogen Energy*, 2023, **48**, 26729-26739.
30. J. Wang, T. H. Nguyen, K. Dong, D. T. Tran, N. H. Kim and J. H. Lee, Engineering dual MoC–Mo<sub>2</sub>C heterostructure–knotted CNTs for efficient direct seawater electrolysis, *International Journal of Hydrogen Energy*, 2024, **49**, 1005-1013.
31. W. Jiang, B. Zhao, Z. Li, P. Zhou, Y. Zhao, X. Chen, J. Wang, R. Yang and C. Zuo, Multihole Ce-doped NiSe<sub>2</sub>/CoP hybrid nanosheets for improved electrocatalytic alkaline water and simulative seawater oxidation, *International Journal of Hydrogen Energy*, 2024, **73**, 590-597.
32. R. Silviya, Y. Vernekar, A. Bhide, S. Gupta, N. Patel and R. Fernandes, Non-Noble Bifunctional Amorphous Metal Boride Electrocatalysts for Selective Seawater Electrolysis, *ChemCatChem*, 2023, **15**.
33. Y.-P. Dong, J.-B. Chen, J. Ying, Y.-X. Xiao, Y. Tian, L. Shen, L. Xia, G. Tian, S.-M. Wu, Y. Lu and X.-Y. Yang, Directional electron transport and strong chloridion repulsion enabled by Hierarchical NiCo<sub>2</sub>O<sub>4</sub>/NiCoP heterojunction for efficient seawater oxidation, *Chemical Engineering Journal*, 2024, **495**.
34. X. Wang, J. Chen, L. Xu, J. Miao, J. Sunarso, X. Wang, W. Cao, Y. Yang and W. Zhou, Electrocatalytic selective oxygen evolution of FeOOH-modified perovskite for alkaline seawater electrolysis, *Journal of Power Sources*, 2024, **614**.

35. M. Saquib, P. Arora and A. C. Bhosale, Nickel molybdenum selenide on carbon cloth as an efficient bifunctional electrocatalyst for alkaline seawater splitting, *Fuel*, 2024, **365**.
36. S. Barua, A. Balčiūnaitė, D. Upskuvienė, J. Vaičiūnienė, L. Tamašauskaitė-Tamašiūnaitė and E. Norkus, Bimetallic Ni–Mn Electrocatalysts for Stable Oxygen Evolution Reaction in Simulated/Alkaline Seawater and Overall Performance in the Splitting of Alkaline Seawater, *Coatings*, 2024, **14**.